Passband shapes that minimize the insertion loss and bandwidth of coupled-resonator bandpass filters

Xinchang Zhang* **and Miloš A. Popović†**

Department of Electrical and Computer Engineering, Photonics Center, Boston University, Boston, MA 02215, USA

**zhangxc@bu.edu, †mpopovic@bu.edu*

Abstract: We use a general theory to show a new class of bandpass filter shapes for coupled-resonator filters that provides the lowest insertion loss and the narrowest bandwidth achievable for a given intrinsic Q and bandwidth.

Bandpass filters are among the most widely used components in integrated photonics across many applications [1–3]. Passband synthesis in higher-order filters provides certain optimum properties such as fastest rolloff rate with given passband restrictions (leading to Butterworth or Chebyshev designs). Such passband synthesis techniques generally assume lossless resonators. In real implementations, finite loss Qs of resonators lead to insertion loss, and also a change in the passband shape from the synthesized response. While Butterworth or Chebyshev passband shape can be recovered by adjusting couplings to compensate for cavity loss Q, the insertion loss increases. This suggests that a rounder passband results in lower insertion loss for a given fixed 3 dB bandwidth filter. A question to ask is whether rounder passband shapes than Butterworth provide a significant insertion loss advantage without significant downsides.

In this paper, we use a second-order filter case study to investigate the insertion loss and narrowest achievable bandwidth and their dependence on the passband shape. While some of the qualitative findings apply more generally to higher orders, a second-order filter has sufficient selectivity yet low enough complexity to be a widely relevant example. These results may benefit loss-sensitive filtering applications such as quantum-correlated photon pair sources and RF-photonic integrated circuits.

To design a second-order filter, we start with a target resonance wavelength and given resonator loss Q. Fig. 1 summarizes the studied device geometry, including the passband shape of proposed filter. The passband spectrum of the filter is fully determined by ring-bus in/out coupling rates r_e and r_d, and ring-ring coupling rate μ with temoral coupled mode theory (CMT). It has been shown that a single-ring filter has maximum drop port transmission *not* under the well known critical coupling condition but when the ring-bus couplings are *symmetric*, that is $r_e = r_d$ [5]. This does not necessarily translate to second-order. To provide a straightforward description of the passband and device geometry we introduce three new parameters that fully specify the filter passband: a shape parameter S (real number, $-\infty < S < +\infty$), the 3-dB bandwidth $\Delta\omega_{3\mathrm{dB}}$, and "impedance match", defined as $M = (r_e - r_d)/(r_e + r_d + 2r_o)$ with $-1 < M < 1$. $M = 0$ corresponds to a symmetric device geometry shown in Fig. 1(a). $M < 0$ ($r_e < r_d$) corresponds to the asymmetric structure in Fig. 1(b). With the possible pole configurations shown by Figs. 1(d),(e) we uniquely characterize the passband shape by shape parameter $S \equiv \tan^2\theta = X^2/Y^2 (S > -1)$. For $\theta = 45^\mathrm{o}$, the pole in Fig. 1(d) makes the filter Butterworth, and $\theta > 45^\mathrm{o}$ (closer to the real axis) are Chebyshev filters with different ripple factors. For $\theta < 45^\mathrm{o}$ (purple area) we see the rounder "sub-Butterworth" passbands. As S decreases from 1 to 0 (sub-Butterworth Type I), the pole path is shown in Fig. 1(e) by the black arrowed curves and the poles coalesce for $S = 0$. When we select $S < 0$ (Type II), X becomes imaginary and the poles split vertically and move in opposite directions along the imaginary axis, as illustrated by the straight arrowed lines in Fig. 1(e).

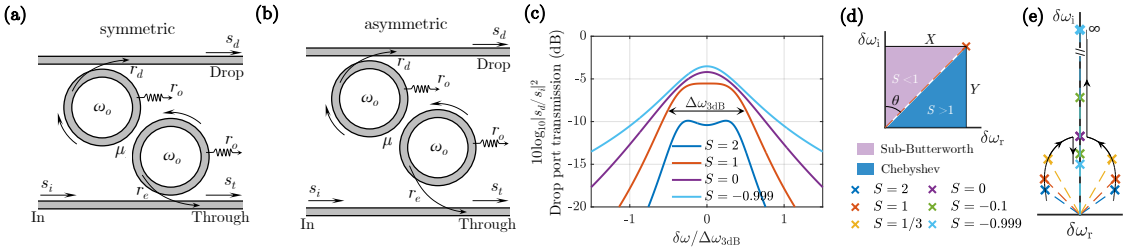

Fig. 1: **Continuum of passband shapes supported by 2nd-order resonant system:** The three design parameters (r_e, r_d, μ) in a synchronous filter are recast in terms of bandwidth $\Delta\omega_{3\mathrm{dB}}$, passband shape S, and impedance matching (a) $M = 0$ (symmetric), or (b) $M < 0$ (asymmetric, $r_e < r_d$). (c) Passband spectra showing different shapes S with fixed 3-dB bandwidth $\Delta\omega_{3\mathrm{dB}}$. (d) One of two symmetric poles of the transmission function, defining shape parameter S. (e) Locus of poles for different passband shapes S. The poles split around an "exceptional point" at $S = 0$.

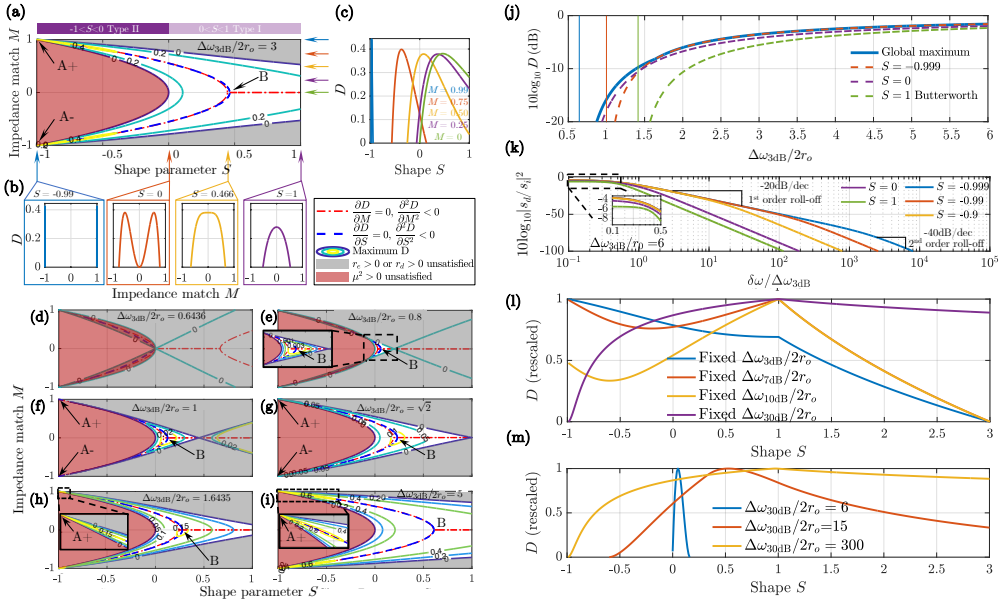

Fig. 2: **Normalized optimum passband design plots and discussions:** Contours of constant peak transmission vs. M and S, for a range of normalized 3 dB bandwidths $\Delta\omega_{3\text{dB}}/2r_o$ (red/gray areas mean non-physical coupling rates). (a) 3 dB bandwidth $\Delta\omega_{3\text{dB}}/2r_o = 3$. (b) Vertical and (c) horizontal slices of (a), showing the peak transmission (b) versus matching M given fixed shape S, and (c) versus shape S given fixed matching M. (d,e) Filters with the narrowest achievable bandwidth have $S = 0$. (f) Bandwidths above which $S = -1$ and (g) $S = 1$ are accessible (all have optimum design at point B). (h) Bandwidth at which global maximum transmission is equal for all three designs A$\pm$ and B; and (i) at which optimum is at $S = -1, M = \pm 1$ (A$\pm$). (j) Optimized peak transmission vs. bandwidth. (k) Bode plots of drop spectra. Re-scaled peak transmission versus shape with (l) sufficiently large bandwidth for different out-of-band rejection level, and (j) ultra-narrow and large 30 dB out-of-band rejection.

The peak transmission from drop port (noted by D) is calculated as a function of S, M under target $\Delta\omega_{3\text{dB}}$ and the results are shown in Fig. 2. There are two sets of (S,M) values, A$\pm$ and B corresponding to local maxima of peak transmissions. As compared in Fig. 2 (e-i), when the normalized bandwdith $\Delta\omega_{3\text{dB}}/2r_o <= 1.6435$, point B is the optimized design for lowest insertion loss. Points A$\pm$ provide lowest insertion loss with asymmetric ring-bus coupling ($M = \pm 1$). When $\Delta\omega_{3\text{dB}}/2r_o = 1.6435$ points A$\pm$ and B provide equal local maxima of transmission.

The narrowest achievable 3 dB bandwidth depends on the opening between gray/red shaded areas. As shown in Fig. 2(e) and (d), the shaded area start to open around $S = 0$ when $\Delta\omega_{3\text{dB}}/2r_o = 0.6436$. Thus, this is the narrowest achievable bandwidth for a 2$^{\text{nd}}$ order filter. The narrowest bandwidth for $S = -1$ [Fig. 2(f)] and $S = 1$ [Fig. 2(g)] are $\Delta\omega_{3\text{dB}}/2r_o = 1$, and $\sqrt{2}$; respectively. These results are also shown in Fig. 2(j) as the vertical lines corresponding to the horizontal intercepts when peak transmission D (in dB) goes to negative infinity for a given shape.

Finally we discuss the roll-off rate of sub-Butterworth filter and generalize the results to N dB out-of-band rejection. As shown in Fig. 1(e), when S approches -1, one of the transfer function pole goes to infinity and this leads to a 1st-order out-of-band roll-off behavior shown in Fig. 2(k). For fixed 3 dB bandwidth, when $\Delta\omega_{3\text{dB}}/2r_o$ is sufficiently large point B converges to Butterworth passband shape $S = 1$. This can be generalized into fixed N dB bandwidth. For $N < 7$, passband shape $S = -1$ provides the lowest insertion loss. Butterworth filter $S = 1$ provides lowest insertion loss when rejection level is higher than 7 dB. However, the red-shaded boundary shown in Fig 2 is independent on bandwidth. That means for any out-of-band rejection level, the filter passband shape with narrowest bandwidth is always around $S = 0$. An example is shown in Fig. 2(m). For fixed 30 dB rejection, the lowest insertion loss of filter with extremely narrow bandwidth ($\Delta\omega_{30\text{dB}}/2r_o = 6$ or 15) is achieved by sub-Butterworth passband shape $S < 1$.

In conclusion, we theoretically demonstrate that a filter with "rounder" passband provides lowest insertion loss. These rounder passband filter also provide narrowest achievable linewidth for abitrary level of signal rejection.

Acknowledgments: This work was funded by NSF ASCENT Award #2,023,751. We thank Manuj Kumar Singh for helpful discussions.

References

1. M. Popović, *et al.*, "Tunable, fourth-order silicon microring-resonator add-drop filters," ECOC (2007), paper 1.2.3.
2. M. Popović, *et al.*, "Multistage high-order microring-resonator add-drop filters," Optics Letters 31, 2571 (2006).
3. C.M. Gentry, *et al.*, "Monolithic source of entangled photons with integrated pump rejection," in Proc. CLEO, paper JTh4C.3, May 2018.
4. D. Onural, *et al.*, "Ultra-high Q Resonators and Sub-GHz Bandwidth Second Order Filters..." in Proc. OFC, paper W1A.4, Mar 2020.
5. M. Dašić and M.A. Popović, "Minimum Drop-Loss Design of ...", in Proc. TELFOR, Belgrade, Serbia, Nov 22, 2012, paper 6.9, p.927.